

C-band dual polarization radar retrieval of rainfall: application of an iterative technique with embedded neural-network

G. Vulpiani¹, E. Picciotti¹, G. Ferrauto¹, F. S. Marzano¹, and V. Chandrasekar²

¹Centro di Eccellenza CETEMPS, Dipartimento di Ingegneria Elettrica e Dipartimento di Fisica, Università dell'Aquila, Italy

²Colorado State University, Fort Collins, Colorado, USA

Abstract. Polarimetric radar measurements at C-band require correction for propagation effects before using them for rainfall retrieval. Since differential phase shift K_{dp} is affected by the spatial variation of the backscattering differential phase shift δ , a new neural-network estimation technique is applied to remove δ effects on K_{dp} estimate. In this study we also explore a new hybrid iterative technique with constraint to correct for attenuation and differential attenuation based on a neural-network scheme and a differential phase constraint. Numerical simulations are used to investigate the efficiency of this approach with respect to others profiling techniques. The simulator is based on a T-matrix solution technique, while the hydrometeor distribution has been characterized with respect to dielectric composition (water, ice and mixed phase), raindrop size distribution (normalized gamma distribution), shape (ellipsoid with parameterized aspect ratio) and angle orientation. A sensitivity analysis is performed in order to evaluate the expected errors of this method to system bias. The performance of these correction procedures and the effects of an error bias on radar measurements are evaluated by using mono-dimensional Gaussian raincell models. Numerical results are discussed in order to show the potential and robustness of the proposed technique.

1 Introduction

For frequencies higher than S band, path attenuation effects due to rainfall can become important and need to be compensated to aim at a quantitative estimation of rainrate. Algorithms using the specific differential propagation phase (K_{dp}) are immune to such effects (Zrnic and Ryzhkov, 1996), but depend on the accuracy of its estimation. As a matter of fact, K_{dp} is the slope of the range profile of differential phase shift (Φ_{dp}), which can be estimated with an accuracy of few degrees.

Correspondence to: G. Vulpiani
(g.vulpiani@aquila.infn.it)

The classic iterative approaches (Hildebrand, 1978; Meneghini, 1978) for attenuation correction, beginning from the first (closest to the radar) range resolution volume and proceeding to successive resolution volumes, are known to be unstable if path integrated attenuation is large. Besides these methods generally assume a power law relation between reflectivity and specific attenuation and that the radar calibration is performed with high accuracy. A great improvement to these attenuation correction procedures is supplied by using the total path-integrated attenuation (PIA) as a constraint.

Recently, the use of Φ_{dp} constraint to estimate the PIA and to correct the measured reflectivity (Z_h) and differential reflectivity (Z_{dr}), proposed and evaluated by Testud et al. (2000) and Le Bouar et al. (2001) respectively, was improved by Bringi et al. (2001) through the use of a self-consistent scheme. The aim of this study is to introduce a new iterative approach with Φ_{dp} constraint to retrieve Z_h and Z_{dr} at attenuating frequencies.

2 Rain backscattering model

Microphysical properties of the rain medium play an important role for radar observations together with the raindrop size distribution (RSD), shape and orientation distributions. In the next paragraphs the rain backscattering model will be briefly described.

2.1 Raindrop size distribution

In 1948 the Marshall-Palmer exponential distribution, having the form $N(D) = N_0 \exp(-\Lambda D)$ with D the particle diameter, has been proposed to describe the spectra of observed drop diameters at weak or moderate rainfall rates (Marshall and Palmer, 1948). Since then, the shape of RSD is matter of discussion in radar meteorology because it rules the relationships between the radar observables and rain rate.

The modified gamma distribution $N(D) = N_0 D^\mu \exp(-\Lambda D)$ (as in Willis, 1984) has been introduced to describe

the deficit of small drops and the convexity of RSD for large drop diameters at high rain rates. In the gamma RSD (which coincides with the exponential one for $\mu = 0$), the parameter N_0 is not considered a physical quantity because its dimension ($[\text{mm}^{-1-\mu} \text{m}^{-3}]$) is μ -dependent.

Recently, to overcome this problem a “normalized” gamma distribution has been introduced by Wiilis (1984) and revisited by Bringi and Chandrasekar (2001), Testud et al. (2001) and Illingworth and Blackman (2002). The number of raindrops per unit volume per unit size (D to $D + dD$) can be written as

$$N(D) = N_w f(\mu) \left(\frac{D}{D_0} \right)^\mu \exp \left[-(3.67 + \mu) \frac{D}{D_0} \right] \quad (1)$$

being

$$f(\mu) = \frac{6}{(3.67)^4} \frac{(3.67 + \mu)^{\mu+4}}{\Gamma(\mu + 4)} \quad (2)$$

where the parameter D_0 is the median volume drop diameter, μ is the shape of the drop spectrum, and N_w [$\text{mm}^{-1} \text{m}^{-3}$] is a normalized drop concentration that can be calculated as function of liquid water content W

$$N_w = \frac{(3.67)^4}{\pi \rho_w} \frac{10^3 W}{D_0^4} \quad (3)$$

The value of this normalization is that it allows the liquid water content to remain constant even if μ changes.

2.2 Axis ratio relationship

The shape of a raindrop can be described by an oblate spheroidal for which, the equivalent volume diameter D_e , is related to the axis ratio a/b by a relation which has been investigated by several authors. In this study we limited our attention on the combination (named AB) of that proposed by Andsager et al. (1999)

$$\frac{a}{b} = 1.012 - 10^{-3} (14.45 D_e + 10.28 D_e^2) \quad (4)$$

used in the interval $1 \text{ mm} \leq D_e \leq 4 \text{ mm}$, and that proposed by Chuang and Beard (1990)

$$\frac{a}{b} = 1.005 + 10^{-4} (5.7 D_e^2 - 260 D_e^2 + 37 D_e^3 - 2 D_e^4) \quad (5)$$

for $D_e \leq 1 \text{ mm}$, $D_e \geq 4 \text{ mm}$.

A raindrop falls in the atmosphere with its symmetry axis aligned in the vertical direction. The canting angle (β) in the polarization plane is defined as the angle measured clockwise between the projection of the symmetry axis of spheroidal particle and the direction running opposite to the vertical one (i.e. $-V$) so that, in case of horizontal incidence, it coincides with the tilt of the particle symmetry axis (e.g. Bringi and Chandrasekar (2001), pp. 68–71). As shown by Beard and Jameson (1983), the distribution of canting angles can be represented by a Gaussian model with zero mean and standard deviation $\leq 5^\circ$.

2.3 Polarimetric radar observables

Computations are done for the 5-cm wavelength, and the gamma distribution is assumed for drop sizes between 0.3 and 8 mm. It is known that big drops often occur in mid-latitude storms. At C-band wavelengths (λ), the transition between Rayleigh and Mie scattering occurs for water drops of about 3 mm. The extension into the resonant scattering region needs use of numerical solution approaches like the T-matrix method to compute the amplitude matrix S , which linearly transforms the electric field components of the incident wave into those of the scattered wave (Mishchenko, 2000; Mishchenko et al., 2000). Rainfall rate R , the radar reflectivity factors ($Z_{hh,vv}$) at H and V polarization state and Z_{dr} , which is the ratio of reflectivity at the two polarization states, can be expressed in term of the RSD as follows:

$$R = 0.6\pi 10^{-3} \int D^3 N(D) v(D) dD \quad (6)$$

$$Z_{hh,vv} = \frac{\lambda^4}{\pi^5 |K|^2} \int 4\pi |S_{hh,vv}^b(D)|^2 N(D) dD \quad (7)$$

$$Z_{dr} = 10 \log \frac{Z_{hh}}{Z_{vv}} \quad (8)$$

where $S_{hh,vv}^b$ are the backscattering co-polar components of S , $K = (\varepsilon - 1)/(\varepsilon + 2)$ being ε the complex dielectric constant of water or ice which is estimated as a function of wavelength and temperature (Ray, 1972), and $v(D)$ is the terminal fall speed in still air.

As derived by Atlas and Ulbrich (1977), $v(D)$ can be expressed using following relationship

$$v(D) = 3.78 D^{0.67} \quad (9)$$

Also the specific differential phase shift (K_{dp}), which is due to the forward propagation phase difference between the two polarization, and co-polar correlation coefficients (ρ_{hv}) can be obtained in terms of the scattering matrix S as:

$$K_{dp} = \frac{180}{\pi} \text{Re} \int [S_{hh}^f(D) - S_{vv}^f(D)] N(D) dD \quad (10)$$

$$\begin{aligned} \rho_{hv} &= \frac{\int S_{vv}^b S_{hh}^{b*} N(D) dD}{\sqrt{\int |S_{hh}^b|^2 N(D) dD \int |S_{vv}^b|^2 N(D) dD}} = \\ &= |\rho_{hv}| e^{j\delta} \end{aligned} \quad (11)$$

where $S_{hh,vv}^f$ are the forward-scattering co-polar components of S and δ (in deg) is the volume backscattering differential phase.

3 Attenuation correction using an iterative approach with embedded neural network

The proposed technique, named Neural Iterative Polarimetric Precipitation Estimation by Radar (NIPPER) is illustrated in the next paragraphs.

As proposed by Testud et al. (2000), it is possible to use the Φ_{dp} constraint to estimate the path-integrated attenuation and differential attenuation. In fact, as scattering simulations have demonstrated (Bringi et al., 1990; Jameson, 1992), A_h and A_{dp} (both expressed in dB km^{-1}) are linearly related to K_{dp} (in $^\circ \text{km}^{-1}$) which is the range derivative of Φ_{dp} . Note that, before applying the attenuation correction scheme the differential phase shift Φ_{dp} must be filtered from the back-propagation effects which are non negligible at C-band (Hubbert and Bringi, 1995).

The suggested algorithm can be described in the following way. As shown in the block diagram in Fig. 1, the first step is the estimation of the path integrated attenuation $PIA_h(r_N)$ (and the path integrated differential attenuation $PIA_{dp}(r_N)$) at the last range r_N by using the Φ_{dp} constraint.

Therefore the corrected values of Z_h and Z_{dr} are derived at the last range volume (here the N^{th})

$$Z_{h,dr}^C(r_N) = Z_{h,dr}^m(r_N) + PIA_{h,dp}(r_N) \quad (12)$$

where the superscripts C and m stand respectively for corrected and measured.

Using the corrected values of Z_h , Z_{dr} , it is possible, through, a back-propagation neural network to estimate the specific attenuation (and the specific differential attenuation) at the N^{th} range volume

$$A_{h,dr}(r_N) = f^{NN}(Z_h^C(r_N), Z_{dr}^C(r_N)) \quad (13)$$

where f^{NN} is Neural Network functional used for the specific attenuation (differential attenuation) estimation.

As a consequence we can estimate the PIA at the $(N-1)^{th}$ range bin as

$$PIA_{h,dp}(r_{N-1}) = PIA_{h,dp}(r_N) - A_{h,dr}(r_N) \cdot \Delta r \quad (14)$$

where Δr is the bin range resolution, while the corrected values of reflectivity and differential reflectivity are

$$Z_{h,dr}^C(r_{N-1}) = Z_{h,dr}^m(r_{N-1}) + 2 \cdot PIA_{h,dp}(r_{N-1}) \quad (15)$$

Generalizing (15) and (16) for the K^{th} range volume, we can write

$$PIA_{h,dp}(r_K) = PIA_{h,dp}(r_N) - \int_{r_N}^{r_K} A_{h,dr}(s) \cdot ds \quad (16)$$

$$Z_{h,dr}^C(r_K) = Z_{h,dr}^m(r_K) + 2 \cdot PIA_{h,dp}(r_K) \quad (17)$$

and so on it is possible to iteratively correct the whole profile of Z_h and Z_{dr} .

At each range volume a control check on Φ_{dp} filtering is performed estimating δg by means of corrected variables using a neural-network algorithm (Vulpiani et al., 2003).

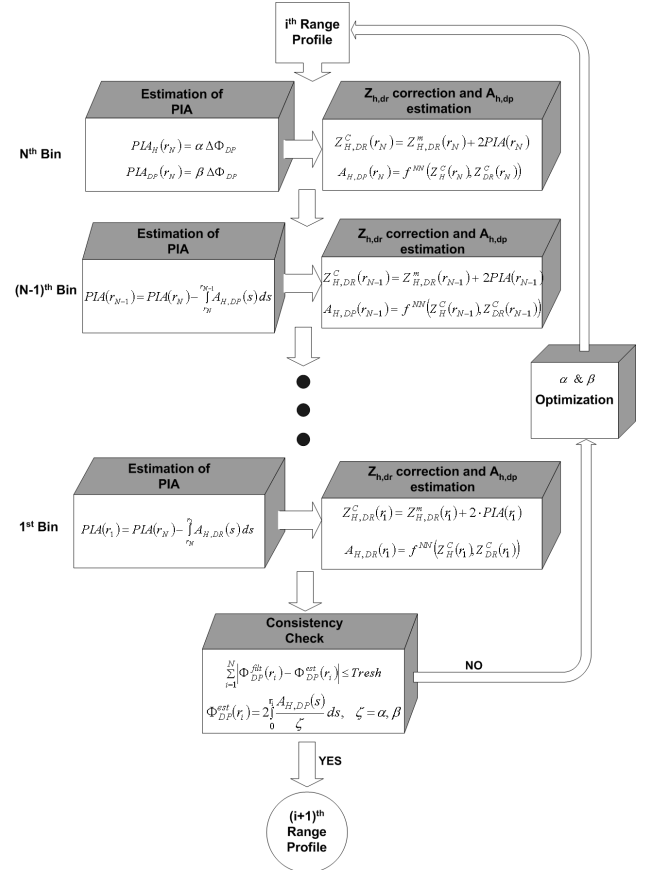


Fig. 1. Block diagram of the proposed attenuation correction scheme.

4 Simulation environment and numerical results

In order to investigate the scattering properties of a rainy medium it is necessary to specify both the incident wave and rainy medium properties. In this study, we limited our attention to C-Band wavelengths and we assumed horizontal incident wave propagation. Concerning to the raindrop size distribution, as anticipated in Sect. 2, we adopted a normalized gamma distribution assuming that D_0 and μ are variable along the path and randomly distributed inside the range proposed by Bringi et al. (2002).

As highlighted by Testud et al. (2002), the intensity of rain can be characterized using the liquid water content W (also named LWC) or the rainfall rate R . In this work we adopted this suggestion so that, assuming a double Gaussian shaped range profile of liquid water content (W [g m^{-3}]), the N_w parameter profile can be obtained using Eq. (3) and the randomly generated values of D_0 as inputs. For each range bin, the axis ratio relationship is selected randomly between the three relationships reported in Sect. 2 according to a uniform distribution. The dielectric constant is dependent on temperature, being fixed the wavelength, and is determined according to scheme proposed by Ray (1972). The numerical scheme adopted to introduce noise on simulated data is that suggested by Testud et al. (2000).

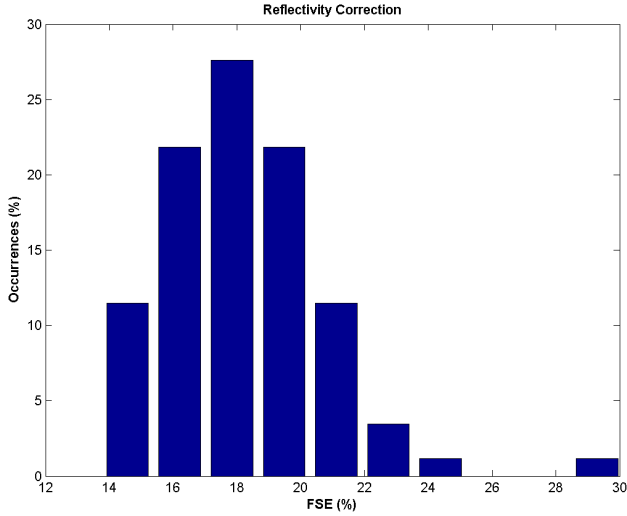


Fig. 2. Comparison between ZPHI and NIPPER for the Z_h correction. The results are evaluated in terms of the histogram of FSE and FME assuming a well-calibrated radar.

4.1 Discussion on algorithm assumptions

The ZPHI algorithm is based on the hypothesis that the exponent β , characterising the relation between reflectivity and attenuation, is constant and N_w is a “local” invariant (e.g. ...“reasonably constant at a scale of some 10 km”, Testud et al., 2000). While scattering simulations have demonstrated that the first one is reasonable in C-band, the second is more questionable. The disdrometer data analysis described in Kozu and Nakamura (1991) showed that, within a given rain regime, the fluctuations of N_0 (the “intercept” parameter of a modified gamma distribution in a logarithmic plane) could be considered “moderate” if compared with the “jumps” occurring in the transition region. Because of the physical similarity between N_0 and N_w (when $\mu = 0$ they coincide), in Testud et al. (2000) the authors expected the same behavior for N_w . Besides, the data collected from the NCAR-Electra PMS probe during the TOGA COARE experiment on 14 December 1992 and analyzed in Testud et al. (2001) confirmed this trend. In such conditions, after the separation of stratiform and convective rain regions, the ZPHI analytical solution can be successfully used through a “segmentation” procedure (e.g. Testud et al., 2000) which provides much more moderate variability of N_w .

Nevertheless, as a result of a case study for a squall-line system passing over a watershed in northern Mississippi presented in Uijlenhoet et al. (2003), the concept of “local” invariance of N_w should be reconsidered. During this event, other than a jump of N_0 (here the intercept parameter of the exponential distribution) in the stratiform-convective transition phase, corresponding to the disappearance of the radar bright band, the authors noticed that “...during the convective phase there is a sudden drop and a new jump, after which N_0 reaches an even larger value than during the transition phase...”. Analyzing the relative behavior of R , Z_h and Z_{dr} they

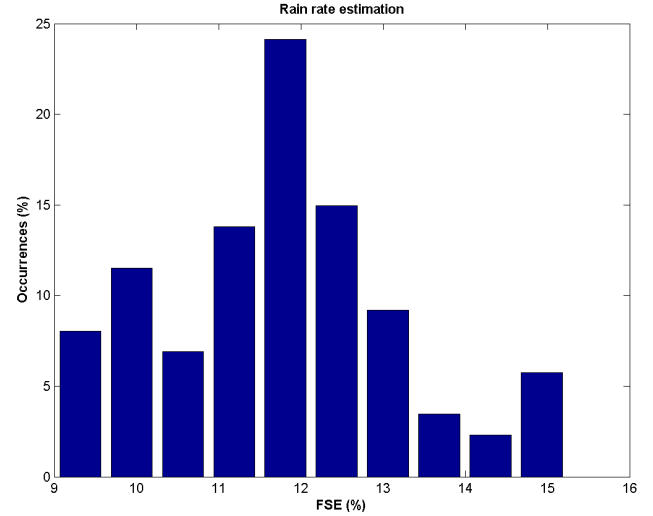


Fig. 3. Performance of the proposed algorithm for rain rate estimation. The results are evaluated in terms of the histogram of FSE.

argued that the observed jump was due to “...a sequence of contrasting regimes within the convective phase of the squall-line system...”. Consequently, the assumption of “moderate” variability inside a specific rain regime has not a general validity and should be carefully used. The use of ZPHI analytical solution could not be suitable showing the dependence from N_w . This is the reason why the NIPPER algorithm can show some advantages in circumstances where there is a significant N_w variability.

4.2 Reconstruction of radar observables

In this subsection we analyze the numerical results obtained applying the proposed attenuation compensation technique to the simulated data set assuming that the radar is well calibrated, remanding the evaluation of the system bias effects to the Subsect. 4.4.

In order to evaluate the performance of the proposed algorithm we define the percentage Fractional Error ε_f as

$$\varepsilon_f = 100 \frac{(Z_{retr}^i - Z_{sim}^i)}{\frac{1}{N} \sum_{i=1}^N Z_{sim}^i} = 100 \frac{\varepsilon}{\langle Z_{sim} \rangle} \quad (18)$$

where the retrieved (Z_{retr}) and simulated (Z_{sim}) reflectivity (or differential reflectivity) are expressed in linear units while the superscript i indicates the number of range bin.

Calculating the root mean square error of the fractional error, we obtain the so-called Fractional Standard Error (FSE) expressed in percentage

$$FSE (\%) = 100 \frac{\sqrt{\langle \varepsilon^2 \rangle}}{\langle Z_{sim} \rangle} = \sqrt{\langle \varepsilon_f^2 \rangle} \quad (19)$$

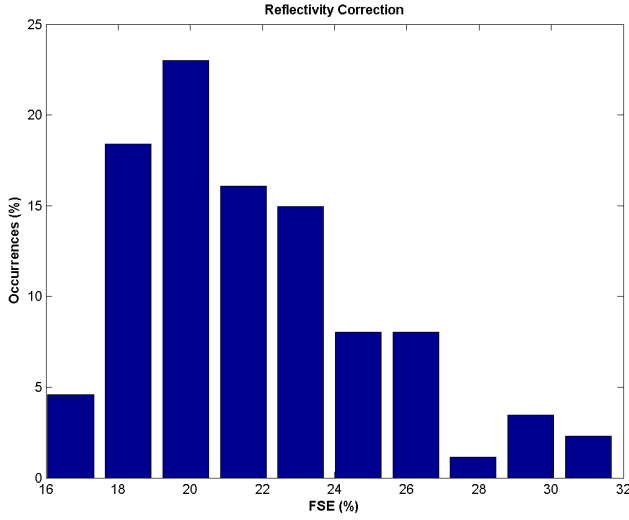


Fig. 4. Comparison between ZPHI and NIPPER for the Z_h correction. The results are evaluated in terms of the histogram of FSE assuming a mis-calibrated radar system (1 dBZ on Z_h).

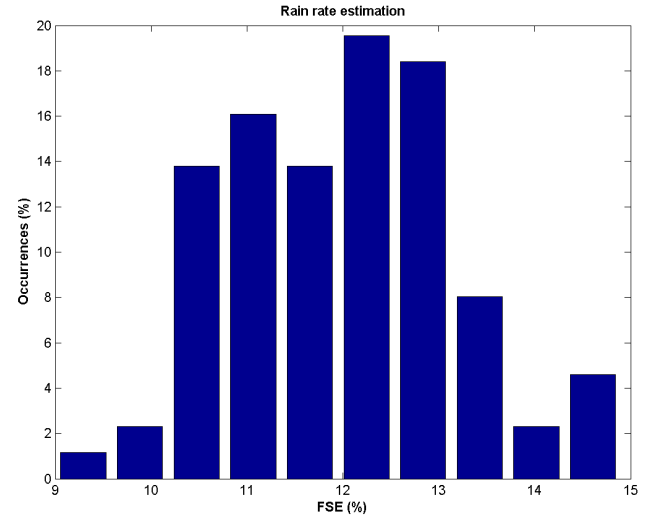


Fig. 5. Performance of the proposed algorithm for rain rate estimation. The results are evaluated in terms of the histogram of FSE assuming a mis-calibrated radar system (1 dBZ on Z_h).

Table 1. Comparison between ZPHI and NIPPER in term of FSE.

FSE (%)	NIPPER		ZPHI	
	Z_h	Z_{dr}	Z_h	Z_{dr}
0 dBZ	18.3	6.2	21.9	6.7
1 dBZ	21.9	5.8	39.6	6.8
2 dBZ	28.0	7.12	76.3	6.5

Table 2. Comparison between ZPHI and NIPPER in term of FME.

FME (%)	NIPPER		ZPHI	
	Z_h	Z_{dr}	Z_h	Z_{dr}
0 dBZ	-2.7	-3.4	-3.8	-3.4
1 dBZ	3.27	-2.6	20.7	-0.7
2 dBZ	8.7	-1.4	51.6	-0.2

Otherwise, calculating the mean of the fractional error, we can define the Fractional Mean Error (FME) expressed in percentage as

$$FME (\%) = 100 \frac{\frac{1}{N} \sum_{i=1}^N (Z_{retr}^i - Z_{sim}^i)}{\frac{1}{N} \sum_{i=1}^N Z_{sim}^i} = 100 \frac{\langle \varepsilon \rangle}{\langle Z_{sim} \rangle} = \langle \varepsilon_f \rangle \quad (20)$$

Figure 2 shows the performances of the ZPHI and NIPPER algorithms in terms of the histogram of FSE and FME calculated for each realization. The same errors indicators, calculated for the whole simulated data set, are shown in Tables 1–2.

The results show that both the algorithms offer good and comparable performances. In case of Z_h retrieval the errors are FSE (%)~21.9 and FME(%)~ -3.8 for ZPHI, and FSE (%)~18.3 and FME(%)~ -2.7 for NIPPER.

4.3 Estimation of rain rate

The main advantage of polarimetric radars is the possibility to use different types of algorithms in order to estimate the rainfall rate. As well as the classical $R(Z_h)$, polarization diversity allows to employ the two parameters algorithm

$R(Z_h, Z_{dr})$ and $R(Z_{dr}, K_{dp})$ other than $R(K_{dp})$. The algorithms using reflectivity and differential reflectivity are affected by radar calibration errors. Otherwise, those using the K_{dp} are conditioned by the differentiation scheme adopted to derive it from Φ_{dp} which is also contaminated by the backscattering differential phase propagation. As a consequence, none these techniques is completely satisfactory. The rainfall estimator proposed in this work (named $R_{NN}(Z_h, Z_{dr})$) is based on a feed-forward neural network with a back-propagation learning algorithm and uses the retrieved profile of Z_h, Z_{dr} . In a formal way, we can write:

$$R_{NN} = f^{NN}(Z_h, Z_{dr}) \quad (21)$$

where f^{NN} is Neural Network functional used for the rain rate estimation. This algorithm, using the potential of neural network, is able to reduce the effects of system noise and to represent complex functions of several variables better than a simple statistical approach.

Figure 3 shows the performance, in terms of FSE, of the proposed rain rate algorithm applied to the corrected values of reflectivity and differential reflectivity. The results are greatly good being FSE(%) less than 12.0 and FME~2.3%.

4.4 Impact of system bias

Bias errors in Z_h and Z_{dr} can affect both the attenuation compensation and the rainfall retrieval algorithms. Typically in a well-maintained radar the bias error on Z_{dr} is less than 0.2 dB while the bias on Z_h is less than 1 dBZ.

Nevertheless, while the bias on differential reflectivity can be estimated and removed easily (Gorgucci et al., 1999), being Z_{dr} a differential power measurement, it is difficult to obtain the absolute calibration of Z_h . For this reason, assuming a bias of 0.2 dB on Z_{dr} , we focused on the impact that the bias on Z_h has on the retrieval of radar observables and on the estimation of rain rate.

As shown in the Tables 1 and 2 and Fig. 4, the proposed technique is quite strong with respect to system bias. Concerning the attenuation correction, the worsening is just about 3.5% in case of 1 dBZ bias and about 10% in case of 2 dBZ bias. On the other side, ZPHI denotes a higher sensitivity to system bias being FSE \sim 39.6% and FME \sim −20.7% while the worsening is about 55% in case of 2 dBZ bias. Moreover, as shown in Fig. 5 it is possible to notice the same efficiency referring to the rain rate estimation using the neural network based algorithm (for the 2 dBZ bias case the FSE remains below 13% while the FME is about 3.1%).

5 Conclusions

Polarimetric radar measurements at C-band require correction for propagation effects before using them for rainfall retrieval.

Since differential phase shift K_{dp} is affected by the spatial variation of the backscattering differential phase shift δ , a new neural-network estimation technique is applied to remove δ effects on K_{dp} estimate. In this study we also explore a new hybrid iterative technique with constraint to correct for attenuation and differential attenuation based on a neural-network scheme and a differential phase constraint. Numerical simulations are used to investigate the efficiency of this approach with respect to others profiling techniques. The simulator is based on a T-matrix solution technique, while the hydrometeor distribution has been characterized with respect to dielectric composition (water, ice and mixed phase), raindrop size distribution (normalized gamma distribution), shape (ellipsoid with parameterized aspect ratio) and angle orientation. A sensitivity analysis is performed in order to evaluate the expected errors of this method to system bias.

The performance of these correction procedures and the effects of an error bias on radar measurements is evaluated by using mono-dimensional Gaussian raincell models. Numerical results are discussed in order to show the potential and robustness of the proposed technique.

Acknowledgement. This work has been partially funded by Italian RAM project of GNDCI-CNR and by Italian Ministry of University and Research (MIUR).

References

- Andsager, K., Beard, K. V., and Laird, N. F.: Laboratory measurements of axis ratios for large rain drops, *J. Atmos. Sci.*, 56, 2673–2683, 1999.
- Atlas, D. and Ulbrich, C. W.: Path- and area-integrated rainfall measurement by microwave attenuation in 1–3 cm band, *J. Appl. Meteor.*, 16, 1322–1331, 1977.
- Beard, K. V. and Jameson, A. R.: Raindrop canting, *J. Atmos. Sci.*, 40, 448–454, 1983.
- Bringi, V. N., Chandrasekar, V., Balakrishnan, N., and Zrni, D. S.: An examination of propagation effects in rainfall on radar measurements at microwave frequencies, *J. Atmos. Ocean. Technol.*, 7, 829–840, 1990.
- Bringi, V. N., Keenan, T. D., and Chandrasekar, V.: Correcting C-band radar reflectivity and differential reflectivity data for rain attenuation: a self-consistent method with constraints, *IEEE Trans. Geosci. Remote Sensing*, 39, 1906–1915, 2001.
- Bringi, V. N. and Chandrasekar, V.: Polarimetric doppler weather radar, Cambridge University Press, 2001.
- Bringi, V. N., Chandrasekar, V., Hubbert, J., Gorgucci, E., Randeu, W. L., and Schoenhuber, M.: Raindrop size distribution in different climatic regimes from disdrometer and dual-polarized radar analysis, *J. Atmos. Sci.*, 60, 354–365, 2002.
- Chuang, C. and Beard, K. V.: A numerical model for the equilibrium shape of electrified raindrops, *J. Atmos. Sci.*, 19, 1374–1389, 1990.
- Gorgucci, E., Scharchilli, G., and Chandrasekar, V.: A procedure to calibrate multiparameter weather radar using properties of the rain medium, *IEEE Trans. Geosci. Remote Sens.*, 37, 269–276, 1999.
- Hildebrand, P. H.: Iterative correction for attenuation of 5 cm radar in rain, *J. Appl. Meteor.*, 17, 508–514, 1978.
- Hubbert, J. and Bringi, V.: An iterative filtering technique for the analysis of copolar differential phase and dual-frequency radar measurements, *J. Atmos. Ocean. Technol.*, 15, 643–648, 1995.
- Illingworth, A. J. and Blackman, T. M.: The need to represent raindrop size spectra as normalized gamma distributions for the interpretation of polarization radar observations, *J. Appl. Meteor.*, 41, 286–297, 2002.
- Jameson A. R.: The effect of temperature on attenuation-correction schemes in rain using polarization propagation differential phase shift, *J. Appl. Meteor.*, 31, 1106–1118, 1992.
- Kozu, T. and Nakamura, K.: Rainfall parameter estimation from dual-radar measurements combining reflectivity profile and path-integrated attenuation, *J. Atmos. Oceanic Technol.*, 8, 259–270, 1991.
- Le Bouar, E., Testud, J., and Keenan, T. D.: Validation of the rain profiling algorithm ZPHI from the C-band polarimetric weather radar in Darwin, *J. Atmos. Ocean. Technol.*, 18, 1819–1837, 2001.
- Marshall, J. S. and Palmer, W. M. K.: The distribution of rain-drops with size, *J. Meteor.*, 5, 165–166, 1948.
- Meneghini, R.: Rain rate estimates for an attenuating radar, *Radio Sci.*, 13, 459–470, 1978.
- Mishchenko, M. I.: Calculation of the amplitude matrix for a non-spherical particle in a fixed orientation, *Appl. Opt.*, 39, 1026–1031, 2000.
- Mishchenko, M. I., Hovenier, J. W., and Travis, L. D.: Light scattering by nonspherical particles, Academic Press, 2000.
- Ray, P. S.: Broadband complex refractive indices of ice and water, *Appl. Opt.*, 11, 1836–1844, 1972.

- Testud, J., Le Bouar, E., Obligis, E., and Ali-Mehenni, M.: The rain profiling algorithm applied to polarimetric weather radar, *J. Atmos. Ocean. Technol.*, 17, 332–356, 2000.
- Testud, J., Oury, S., Black, R. A., Amayenc, P., and Dou, X.: The concept of “normalized” distribution to describe raindrop spectra: A tool for cloud physics and cloud remote sensing, *J. Appl. Meteor.*, 40, 1118–1140, 2001.
- Uijlenhoet, R., Steiner, M., and Smith, J. A.: Variability of raindrop size distribution in a squall line and implications for radar rainfall estimation, *J. Hydrometeor.*, 4, 43–61, 2003.
- Vulpiani, G., Picciotti, E., Ferrauto, G., and Marzano, F. S.: Sensitivity Analysis of Self-Consistent Polarimetric Rain Retrieval to C-Band Radar Observables, *Proc. of IGARSS03*, Toulouse, 2003.
- Willis, P. T.: Functional fit to some observed drop size distribution and parametrization of rain, *J. Atmos. Sci.*, 41, 1648–1661, 1984.
- Zrnica, D. S. and Ryzhkov, A.: Advantages of rain measurements using specific differential phase, *J. Atmos. Ocean. Technol.*, 13, 454–464, 1996.